

SiC/SiC_{woven} fabric laminates: Design, manufacturing, mechanical properties

Nina Orlovskaya^{a,*}, Mykola Lugovy^b, Frank Ko^b, Sergey Yarmolenko^c,
Jag Sankar^c, Jakob Kuebler^d

^a Department of Materials Science and Engineering, Michigan Technological University, 1400 Townsend Drive, Houghton, MI 49931, USA

^b Department of Materials Science and Engineering, Drexel University, Philadelphia, PA, USA

^c North Carolina A&T State University, Greensboro, NC, USA

^d EMPA, Lab for High Performance Ceramics, Duebendorf, Switzerland

Received 28 February 2005; received in revised form 7 July 2005; accepted 15 July 2005

Available online 3 April 2006

Abstract

The SiC/SiC_{wf} laminate design has been targeted to achieve increased residual compressive stress in thin SiC_{wf} layers and small residual tensile stress in thick SiC layers, that would lead to a significant increase of the apparent fracture toughness of the composite. The laminates have been manufactured using rolling and hot pressing techniques. The measured apparent fracture toughness of laminates showed a significant increase over the monolith SiC ceramics. Thus, while the intrinsic fracture toughness of pure SiC ceramics is in the range of 2–3 MPa m^{1/2}, significant increase up to 6–8 MPa m^{1/2} was achieved for the layered ceramics. A crack shielding by compressive residual stress was a main mechanism responsible for the significant toughening of the SiC/SiC_{wf} laminate.

© 2006 Elsevier Ltd. All rights reserved.

Keywords: A. Laminates; B. Fracture toughness; C. Computational modelling; D. Mechanical testing; Silicon carbide woven fabric

1. Introduction

Ceramic composites are important engineering materials with many useful properties. One of the promising applications of ceramics is for armor materials due to low density, superior hardness and high compressive strength values relative to metals. Among the required mechanical properties of ceramics only the fracture toughness has relatively low values for a widespread usage. One way to overcome the brittleness of the ceramics is to design ceramic layered composites with controlled thermal residual stresses. The latest developments in ceramic composites show that the use of layered materials is perhaps the most promising method to control cracks and brittle fracture by deflection, microcracking or internal stresses [1]. It has been shown that residual compressive stresses of ~500 MPa in a surface layer of a three layered alumina–zirconia composite with a strong interface can increase the apparent fracture toughness by a factor of 7.5 (up to 30 MPa m^{1/2}) for crack lengths equal to the surface layer thickness [2]. In our recent work [3], the effect of macroscopic

residual stresses on the fracture resistance and stable/unstable crack growth in Si₃N₄/Si₃N₄–30 wt%TiN layered ceramics has been investigated. Apparent fracture toughness was calculated as a function of the crack length for the laminates with residual compressive or tensile stresses in the top layers. It was shown that for Si₃N₄/Si₃N₄–30 wt%TiN laminates with top Si₃N₄ layers with compressive residual stress the apparent fracture toughness increases from 3.9 to 17 MPa m^{1/2} as a function of the crack length. The experimentally measured apparent fracture toughness values showed an excellent fit with the calculated data. Therefore, it is clear that the residual compressive stress can result in a significant increase in toughness of ceramics. As a result the laminates with strong interfaces, combined with improved fracture toughness and damage tolerance, can potentially provide increase in other mechanical properties, such as ballistic performance, for example.

Silicon carbide is an important ceramic material with many useful physical and chemical properties. Due to its high hardness, this ceramics is a very promising material for ballistic protection. However, SiC-based composites have a relatively low fracture toughness of only 3–4 MPa m^{1/2}. While high hardness is one of the very important indicators for a material's ballistic potential, toughness might play an equally important role in realizing that potential. Thus, materials with both high hardness and high fracture toughness are expected

* Corresponding author.

E-mail address: norlovsk@mtu.edu (N. Orlovskaya).

Table 1
Design parameters

Design	Layer thickness (μm)		Calculated residual stress (MPa)		Fitted residual stress (MPa)	
	SiC _{wf}	SiC	SiC _{wf}	SiC	SiC _{wf}	SiC
1	458	2598	−281	66	−144	34
2	458	1734	−257	91	−132	46
3	458	1397	−242	106	−124	54

to yield the best ballistic performance [4,5]. Therefore, a significant increase in fracture toughness of silicon carbide based laminates has the potential for realization of improved armor material systems.

Brittleness of silicon carbide ceramic laminates can be controlled by designing the distribution of residual stresses, i.e. by placing the layers with high compressive stresses into the bulk of the material. The enhancement of the mechanical performance of SiC based ceramics can be achieved through the design of layered structures with controlled residual stresses in separate layers. One of the novel approaches is to use the SiC woven fabric (SiC_{wf}) with less coefficient of thermal expansion (CTE) as tough thin layers with residual compressive stress while using thick SiC layers produced from powders in order to decrease the residual tensile stress. The goal of this research is to achieve a significant improvement of apparent fracture toughness of SiC/SiC_{wf} ceramic laminates. The manufacturing steps of SiC/SiC_{wf} ceramic laminates, as well as design parameters along with fracture toughness testing results are presented in this paper.

2. Design

The proposed design targets a fracture toughness increase of SiC/SiC_{wf} laminates and is based on the preliminary results both from our work [6–8] and from the work of others [9–12]. We used the design algorithm presented in [13]. Three different macrostructures are considered in this work. The basic condition was that the symmetric macrostructure had been considered with layers consisting of two different components—pure SiC ceramics and SiC_{wf}. SiC_{wf} was placed in the external layers of the laminates. The sign and value of the bulk residual stresses depends on the coefficients of thermal expansion of the materials used as the separate layers and the relative thickness of layers with compressive and tensile residual stresses. For silicon carbide there is wide range of CTE values presented in different works [14,15]. However, our

analysis shows the CTE of SiC fibers containing in SiC woven fabric is typically less than CTE of polycrystalline SiC, which results from a specific crystalline texture of fibers and their phase composition. CTEs of SiC and SiC_{wf} were chosen as 4.7 and $4.4 \times 10^{-6} \text{ K}^{-1}$, respectively [14,15]. These values are approximate and for design estimation only. Such choice leads to the appearance of tensile residual stress in SiC layers and compressive residual stress in SiC_{wf} layers after sintering. There are uncertainties in the calculation of the thermal residual stresses using literature values of CTEs, since CTEs for our materials can be slightly different. However, since no measurements were done for these ceramics, we used the available data for similar materials. The thickness of SiC and SiC_{wf} layers as well as calculated values of thermal residual stresses for three designs are presented in Table 1, and the schematic presentation of the SiC/SiC_{wf} composites is shown in Fig. 1. All three macrostructures used total seven layer composites but while the thickness of SiC_{wf} layers was kept constant, the thickness of SiC layers increased from 1397 to 2598 μm . Such changes in the thickness of SiC layers lead to a calculated residual tensile stress of only 66–106 MPa in SiC and 242–281 MPa residual compressive stress in SiC_{wf} layers, respectively. The ‘joining temperature’ [15] required to calculate the thermal residual stresses was adopted to be a hot pressing temperature of 2423 K, since it is a solid state sintering, therefore, the residual stresses should appear when the cooling of the ceramics starts.

3. Manufacturing procedures

α -SiC powders with a grain size of 2–5 μm were used for the manufacturing of SiC layers. SiC powders were ball milled in acetone in a polyethylene bottle using SiC milling media for 48 h in order to reach a particle size of less than 1 μm . The SiC tapes were produced by cold rolling with a crude rubber (1 wt%) added to the milled and dried SiC powders as a plasticizer through a 3% solution in petrol. The powders were

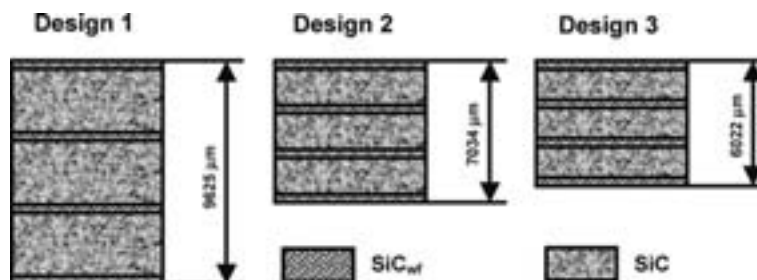


Fig. 1. A schematic presentation of SiC/SiC_{wf} laminate designs.

further dried up to 2 wt% petrol in the mixture. After sieving the SiC powder with a 500 μm sieve, the granulated powder was dried up to 0.5 wt% of residual petrol. A roll mill with 40 mm rolls was used for rolling. The velocity of rolling was in the range of 1–1.2 m/min. The estimated working pressure was 100 MPa to achieve 74% density of the tapes. Thickness of the tapes was about 450 μm after rolling.

A schematic presentation of the laminates manufacturing process is shown in Fig. 2(a). Samples of SiC/SiC_{wf} laminates were prepared by hot pressing of stacked SiC tapes and SiC woven fabric layers. The schematic presentation of the SiC woven fabric is shown in Fig. 2(b). Each of the SiC bundles (Fig. 2(c)) consists about 500 individual SiC fibers (Fig. 2(d)) with a diameter of 15–30 μm . The fibers have inhomogeneous areas that are enriched in C, as was detected by Electron Dispersive Spectroscopy (EDS). In order to achieve the desired thickness of SiC layers, a certain number of thin SiC rolled tapes were stacked together. After the required thickness was achieved, the layer of SiC_{wf} was

placed, followed by the next layer of SiC. The first and the last layers have always been SiC_{wf}. After the assembling of the required layered structure the hot pressing was performed at a heating rate of 100 K/min. The temperature and pressure were kept at 2423 K and 30 MPa, respectively. The dwell time at hot pressing temperature was 50 min. Graphite dies were used for the hot pressing of laminates with the graphite surface coated by BN in order to prevent a direct contact between graphite and ceramic material. Tiles 35 \times 50 mm² were produced.

The specimens for mechanical tests were prepared by machining of the hot pressed tiles. Standard bars of 50 mm length were cut, machined and chamfered along the long edges with a chamfer angle of 45° to a dimension of 0.12 ± 0.03 mm. The fracture toughness was measured by the Single Edge V Notch Beam (SEVNB) technique [16,17]. The V-notches were made in the specimen with a diamond saw, followed by polishing with a diamond paste coated stainless steel blade to obtain a sharp tip for the notch with a tip radii of 3–5 μm .

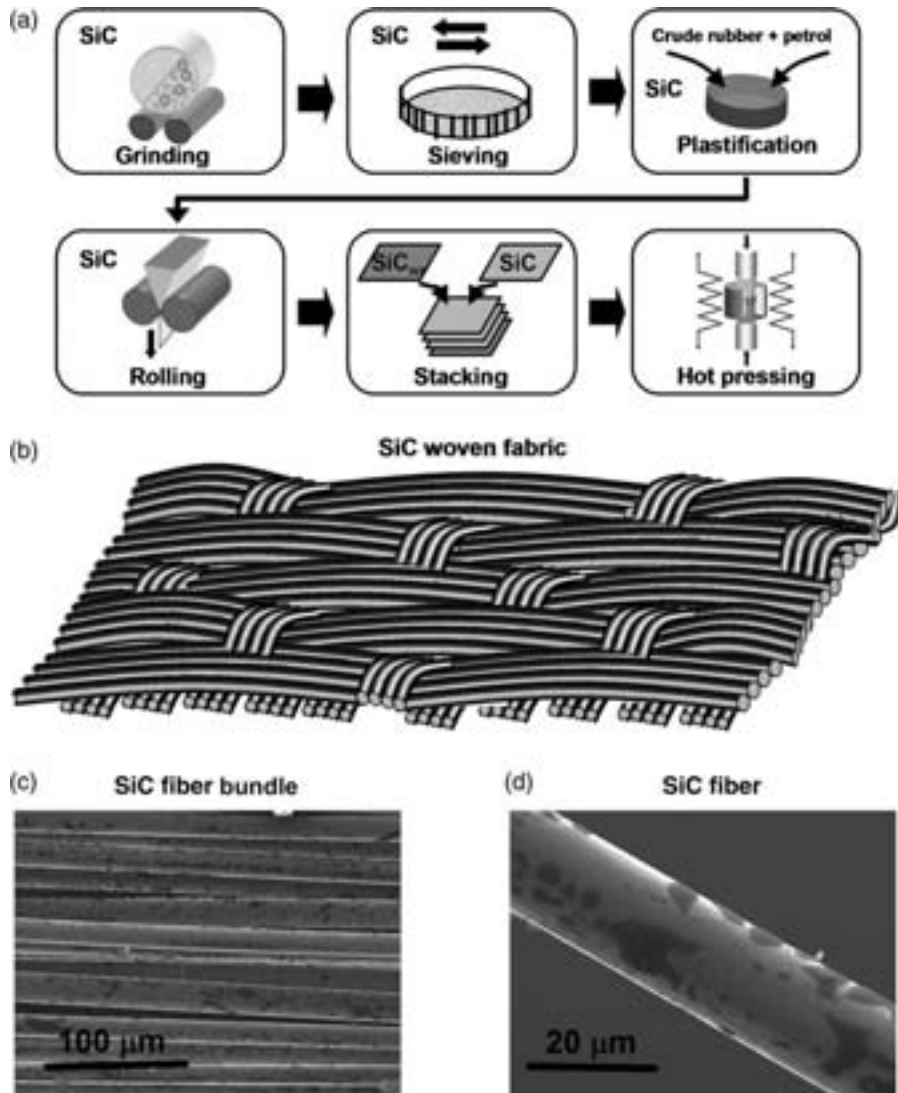


Fig. 2. A schematic presentation of the laminates manufacturing steps (a) and SiC woven fabric (b), SiC fiber bundle (c), SiC fiber (d). The SEM images show the SiC_{wf} bundle and a single SiC fiber. The dark areas at the fiber surface are C enriched spots.

4. Apparent fracture toughness

The measured apparent fracture toughness of the three designed SiC/SiC_{wf} laminates is presented in Fig. 3(a). For comparison the fracture toughness of pure SiC is also shown. The data for SiC ceramics were compiled from the Ref. [14]. As one can see from Fig. 3(a), a significant increase in apparent

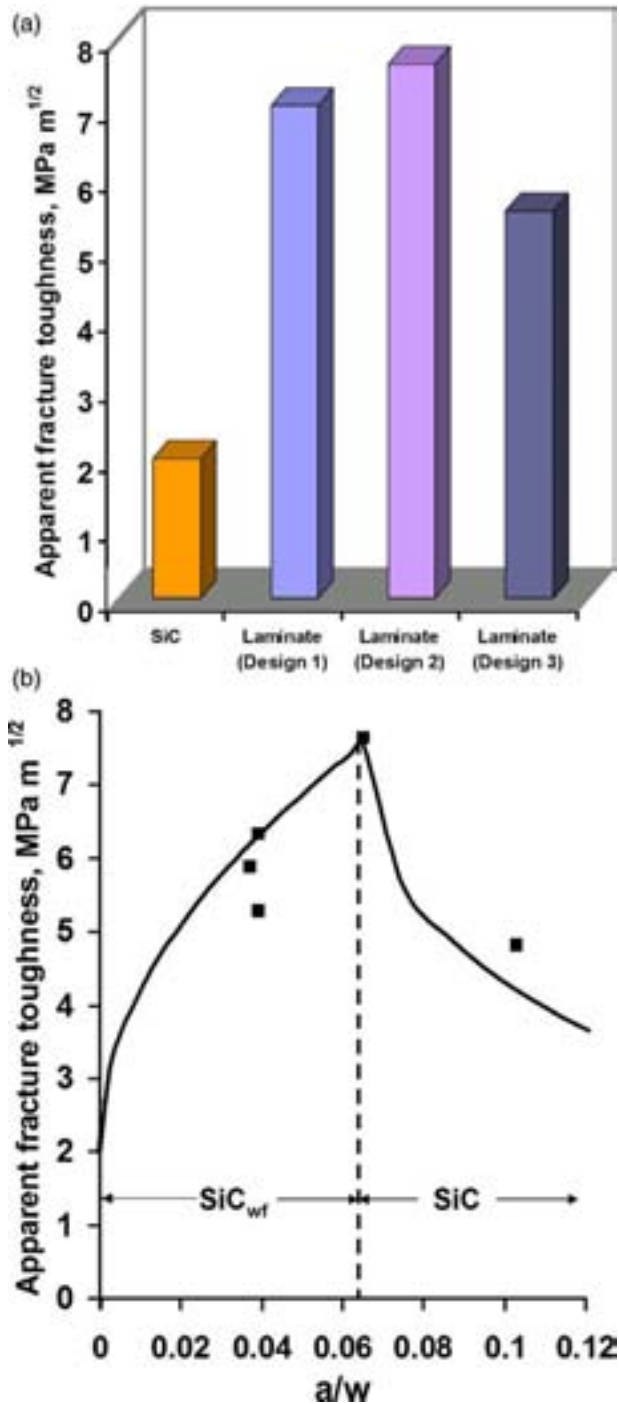


Fig. 3. (a) The maximum apparent fracture toughness values measured for SiC/SiC_{wf} laminates of Designs 1, 2, and 3. For comparison SiC fracture toughness values is also presented. (b) Apparent fracture toughness vs relative crack length (where a is the crack length and w is the total thickness of a sample) for specimens of Design 2.

fracture toughness of layered SiC/SiC_{wf} composites was achieved with respect to pure SiC.

In order to estimate the effect of crack length on the apparent fracture toughness, different notch lengths were cut for the different samples of the Design 2. A total of five samples were tested, where three notches were made with a notch tip ending in the top SiC_{wf} layer. One notch was cut through the whole length of the SiC_{wf} layer to reach the first SiC/SiC_{wf} interface and the last notch tip was placed in the SiC layer. The calculated values of the apparent fracture toughness as a function of the crack length normalized by the total sample thickness for the SiC/SiC_{wf} laminate of Design 2 are shown in Fig. 3(b). The toughness increases in the SiC_{wf} top layer with compressive stress with increasing crack length, and it decreases in the SiC layer with tensile stress as the crack continues to grow. For the SiC_{wf} top layer with compressive stress, the calculated apparent fracture toughness increases from 2 to 7.6 MPa m^{1/2} as a function of the crack length. The apparent fracture toughness reaches its maximum value as the crack approaches the interface, shown as a dashed line in Fig. 3(b), with the SiC layer. The experimentally measured fracture toughness values, also presented in Fig. 3(b), shows an excellent fit with the calculated ones. The maximum apparent fracture toughness was measured when notch tip was at the interface between first SiC_{wf} and first embedded SiC layer.

The one problem was accounted that if the approximate values of CTEs 4.7 and $4.4 \times 10^{-6} \text{ K}^{-1}$ for SiC and SiC_{wf}, respectively, were used [14,15] for the calculation of the residual stresses, the calculated apparent fracture toughness appeared to be much higher than the experimentally measured values. Therefore, to allow a fitting of calculated and measured fracture toughness, the second set of the fitted residual stresses was calculated (Table 1) that lead to an excellent fit with the experimental results. The residual stresses that allow an excellent fit to the experimental fracture toughness data are two times lower than initially calculated thermal residual stresses. Such discrepancies could be explained by the difference in the CTEs used for stress calculation and existing in the real materials.

5. Fracture surface and microstructure

An optical micrograph of SiC/SiC_{wf} sample (Design 1) after failure during fracture toughness measurement is shown in Fig. 4. Obviously, no phase contrast between SiC and SiC_{wf} can be seen by optical imaging and, therefore, layers cannot be distinguished. However, the difference in layers structure can be seen with scanning electron microscopy (SEM). For a given sample bifurcation during crack propagation was observed. The crack started to bifurcate when it reached the centerline of the second SiC_{wf} layer that was under compressive stress. After bifurcation two newly formed cracks crossed the thick SiC layer with residual tensile stress at an angle of 45°. There are compressive curls formed as the crack deflected into the SiC_{wf} centerline just before complete failure of the sample. While crack bifurcation was observed for Design 1 samples, no bifurcation was detected for the two other designs.

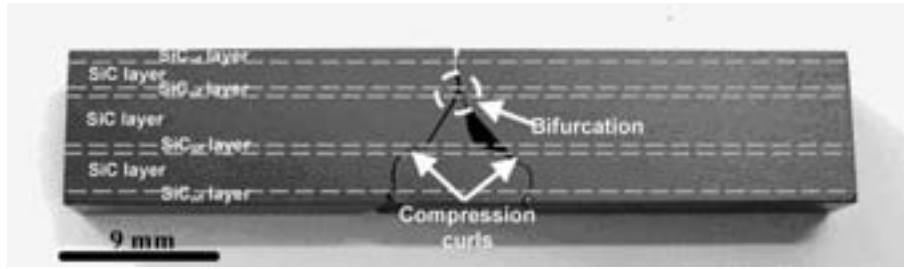


Fig. 4. A crack bifurcation in the laminate of Design 1.

The critical thickness necessary for bifurcation follows a relationship [10,18]

$$l_c = \frac{G_c E}{0.34(1-\nu^2)\sigma_r^2}$$

where G_c , E , and ν are the critical strain energy release rate, Young's modulus, and Poisson's ratio of the compressive layer

material, respectively, σ_r the magnitude of residual compression within the compressive layer, and 0.34 a dimensionless parameter determined by numerical analysis. It should be noted that $G_c E / (1 - \nu^2) = K_c^2$. Here, K_c is the intrinsic fracture toughness of the compressive layer. Then the critical thickness is

$$l_c = \frac{K_c^2}{0.34\sigma_r^2}$$

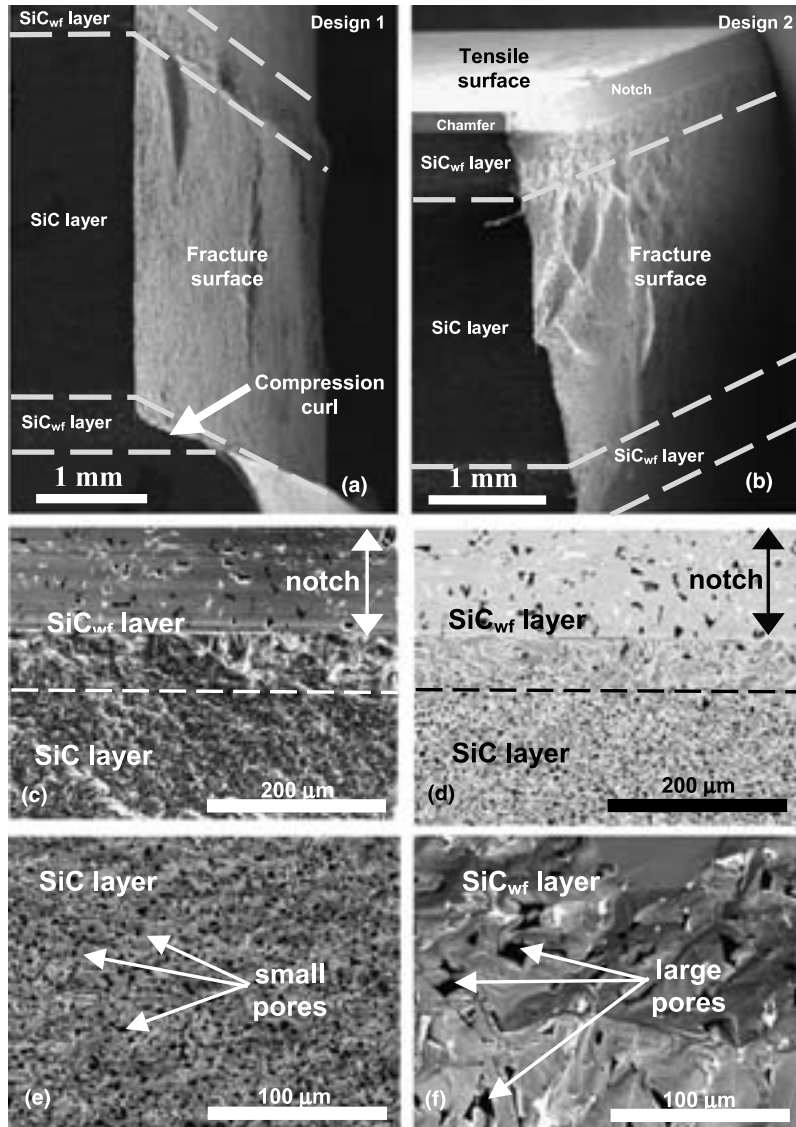


Fig. 5. SEM images of fracture surfaces of SiC/SiC_{wf} laminates: (a) Design 1, (b) Design 2, (c) and (d) a notch in the top SiC_{wf} layer, (e) SiC layer with residual tensile stress, (f) SiC_{wf} layer with residual compressive stress. a, b, c—Secondary electron images; d, e, f—Backscattered images.

Agreement is further improved when the dimensionless parameter is reduced from 0.34 to 0.17 [18]. The critical thicknesses of SiC_{wf} layer to bifurcate are 1134, 1350 and 1530 μm for Designs 1, 2 and 3, respectively, if we use $K_c = 2 \text{ MPa m}^{1/2}$, dimensionless parameter of 0.17 and fitted compressive residual stresses. It means that the bifurcation should not occur in these samples. In fact, there is only one specimen of Design 1, which demonstrated bifurcation (Fig. 4). The possibility is that this sample has random local differences from the other samples, such as defects, or amount of porosity, or other technologic defects. Such differences can lead to decrease in fracture toughness of the material. For example, decreasing fracture toughness of SiC_{wf} layer to $1.27 \text{ MPa m}^{1/2}$ can result in the appearance of crack bifurcation in samples of Design 1. It should be noted that the bifurcation has small effect on the apparent fracture toughness increase, but it could be useful as an additional mechanism of toughening.

Fracture surfaces of SiC/SiC_{wf} samples (Designs 1 and 2) after fracture toughness tests are shown in Fig. 5(a and b), respectively. The compression curl is seen in more details in Fig. 5(a). The notch placed in the top SiC_{wf} layer as well as rather rough fracture surface of SiC layer are presented in Fig. 5(b). One top SiC_{wf} layer and thick first SiC layer with the notch being in the top layer are shown in Fig. 5(c–f). As one can see from the images, a certain amount of residual porosity remains both in SiC_{wf} and rolled SiC layers with a pore size of 5–15 μm in SiC_{wf} layer, and smaller porosity of 2–5 μm homogeneously distributed in SiC layer. No interfaces have been observed between SiC stacked tapes after hot pressing. Only SiC/SiC_{wf} interfaces can be detected on the fracture surface. It seems that no SiC woven fabric structure remains after hot pressing of the laminates, instead rather coarse elongated SiC grains with a grain size up to 100 μm are shown in Fig. 5(f). Small amount of Fe inclusions, as found by EDS, were detected inside some pores in SiC_{wf} layer, which might appear due to Fe contamination of the SiC during rolling. Some Fe particles were detected on SiC tapes after rolling. During the hot pressing these particles were melted and further segregated in SiC_{wf} layers inside pores; however, almost no such inclusions were detected inside the SiC layers.

6. Conclusions

Tough SiC/SiC_{wf} laminates have been developed by designing increased residual compressive stress in thin SiC_{wf} layers and low residual tensile stresses in thick SiC layers. Rolling and hot pressing have been used to manufacture laminates with three different designs. More than twice increase in the apparent fracture toughness was achieved for the SiC/SiC_{wf} layered materials in comparison with pure monolith SiC ceramics. Such an increase can be explained by the significant influence of the residual compressive stresses on the crack propagation during composite loading. The compressive stress acts as a crack shield and is able to significantly increase load required to reach failure. In addition, a crack bifurcation during the laminate failure was also observed, that could also contribute to the toughening of the SiC/SiC_{wf} ceramics. The disagreement between calculated and measured apparent fracture toughness values has lead to

necessity to perform fitting procedures to recalculate possible residual stresses in SiC and SiC_{wf} layers. After such fitting, the calculated and measured data showed an excellent fit. Such discrepancies could be explained by differences in the CTEs of SiC and SiC_{wf} ceramics used in calculations and CTEs of real materials used for laminate manufacturing.

Acknowledgements

The work was supported by the European Commission, the project 1CA2-CT-2000-10020 Copernicus-2 and by AFOSR, the project No. F49620-02-0340. This work was also partly performed at the Army Center for Nanoscience and Nanomaterials, North Carolina A&T State University.

References

- [1] Lugovy M, Slyunyayev V, Subbotin V, Orlovskaya N, Gogotsi G. Crack arrest in Si₃N₄-based layered composites with residual stress. *Compos Sci Technol* 2004;64(13/14):1947–57.
- [2] Blattner A, Lakshminarayanan R, Shetty DK. Toughening of layered ceramic composites with residual surface compression: effect of layer thickness. *Eng Fract Mech* 2001;68:1–7.
- [3] Lugovy M, Slyunyayev V, Orlovskaya N, Blugan G, Kuebler J, Lewis M. Apparent fracture toughness in Si₃N₄-based laminates with residual compressive or tensile stresses in surface layers. *Acta Mater* 2005;53:289–96.
- [4] Sternberg JS. Materials properties determining the resistance of ceramics to high velocity penetration. *J Appl Phys* 1989;69:3417–24.
- [5] Wilkens ML. Mechanics of penetration and perforation. *Int J Eng Sci* 1978;16:793–807.
- [6] Yaroshenko V, Orlovskaya N, Einarsrud M.-A, Kovylayev V. Processing of multilayered Si₃N₄-TiN hot-pressed ceramic composites. In: *Proceedings of NATO ARW 'multilayered and fibre-reinforced composites: problems and prospects'*. Dordrecht, Kluwer; 1998.
- [7] Orlovskaya N, Kuebler J, Subbotin V, Lugovy M. Design of Si₃N₄-based ceramic laminates by the residual stresses. *J Mater Sci* 2005;40:5443–50.
- [8] Lugovy M, Orlovskaya N, Slyunyayev V, Gogotsi G, Kuebler J, Sanchez-Herencia A. Crack bifurcation features in laminar specimens with fixed total thickness. *Compos Sci Technol* 2002;62:819–30.
- [9] Rao MP, Sanchez-Herencia AJ, Beltz GE, McMeeking RM, Lange FF. Laminar ceramics that exhibit a threshold strength. *Science* 1999;286:102–5.
- [10] Oechsner M, Hillman C, Lange F. Crack bifurcation in laminar ceramic composites. *J Am Ceram Soc* 1996;79:1834–8.
- [11] Green D, Cai P, Messing G. Residual stresses in alumina–zirconia laminates. *J Eur Ceram Soc* 1999;19:2511–7.
- [12] Lakshminarayanan R, Shetty DK, Cutler RA. Toughening of layered ceramic composites with residual surface compression. *J Am Ceram Soc* 1996;79:79–87.
- [13] Orlovskaya N, Lugovy M, Subbotin V, Radchenko A, Adams J, Chheda M, et al. Robust design and manufacturing of ceramic laminates with controlled thermal residual stresses for enhanced toughness. *J Mater Sci* 2005;40:5483–90.
- [14] Ceramic tool materials. Gnesin, Kiev GG, editors. *Tekhnika*; 1991 [in Russian].
- [15] Yoshida K, Imai M, Yano T. Improvement of the mechanical properties of hot-pressed silicon–carbide–fiber-reinforced silicon carbide composites by polycarbosilane impregnation. *Compos Sci Technol* 2001;61:1323–9.
- [16] Kuebler J. *Ceram Eng Sci Proc* 1997;18:155–62.
- [17] Kuebler J. In: Jenkins MG, Quinn GD, editor. *ASTM STP 1409*, J.A. Salem. West Conshohocken, PA, ASTM, ISBN 0-8031-2880-0; 2002. p. 93.
- [18] Rao M, Lange FF. Factors affecting threshold strength in laminar ceramics containing thin compressive layers. *J Am Ceram Soc* 2002;85:1222–8.